High speed synchrotron X-ray imaging of ultrasonic bubble cloud in liquid metal

C.Wang[1], D.Tang[1], W.Zhang[1], W. Du[1], T.Connolley[2], J. Mi[1]

[1]School of Engineering, University of Hull, Cottingham Road, Yorkshire, HU6 7RX, UK;
[2]Diamond Light Source, Didcot, Oxfordshire, OX11 0DE, UK

Chuangnan.wang@hull.ac.uk

Abstract. This paper presents the real-time and in-situ synchrotron X-ray high speed imaging studies of ultrasound bubbles and bubble cloud in a liquid Sn-30%Cu alloy. The collective behaviour of the ultrasound bubbles generated by ultrasound powders of 60 W and 100W were successfully captured. The number density of the individual bubbles and the density of the continuous bubble cloud were calculated from the information extracted from the images sequences and presented for the first time for the liquid Sn-30%Cu alloy.

1. Introduction

Ultrasound has found wide applications in science and industry, for example, ultrasound based imaging and non-destructive testing of materials, ultrasound based materials processing, cleaning or welding and ultrasound enhanced chemical reactions (sonochemistry). Among the many applications of ultrasound in a liquid medium, ultrasound induced bubbles and cavitation [1, 2] play very important roles in enhancing the transfer or exchange of mass and energy within the processed medium. However, the behaviour of ultrasonic bubbles and cavitation and their interactions with different materials is not fully understood. This is especially the case for high viscosity, high temperature, opaque liquid media, such as liquid metal alloys. Ultrasonic processing has been proven as an effective method for refining the solidification microstructures for metal alloys [3], but the underlying mechanisms are still under debate. Hence, there is ongoing, intensive worldwide research into how ultrasound bubbles and cavitation interact with liquid metals and their solidifying phases in different alloy systems [3]. Mi. *et al.* have recently used synchrotron X-rays to investigate, in real time, the interactions of ultrasound waves, bubbles with liquid metal and particles [4-6]. In these papers, the dynamics of a single bubble and its interaction with a solidifying particle at the solid-liquid interface were clearly presented. However, many ultrasound bubbles are often created simultaneously when the ultrasound power is over a certain criteria. Therefore, the collective behaviour of those bubbles has more practical significance for any potential industrial applications, and such studies in liquid metals have not been reported.

This paper presents the *in-situ* high speed synchrotron X-ray imaging studies of ultrasound bubble clouds in a liquid Sn-30%Cu alloy. The distribution of the ultrasonic bubbles and the bubble flux in liquid Sn-30%Cu alloy are presented for the first time.

2. Experiment

The experiment was carried out at the I12 beamline at Diamond Light Source, UK. Hull University's apparatus for *in-situ* experiments, consisting of a custom-made sample cell, furnace and ultrasound system, was placed on the beamline. Real-time, high speed X-ray images of ultrasound processing of a liquid alloy were then obtained using the beamline's imaging system.

2.1. Alloy, Sample and Ultrasound

Sn-30wt%Cu alloy was chosen as the experimental alloy because Sn has a melting point of just 231.93 °C, and it is an ideal candidate as the liquid metal matrix for applying ultrasound over a wide range of temperatures, from 250 to 750 °C. Furthermore, the Sn-Cu binary system [7] is the key alloy system for lead-free soldering materials, and intermetallic compounds such as Cu_6Sn_5 are promising candidates for enhancing the storage capacity of Lithium ion based batteries [3].

A special quartz tube with a thin window in the middle was used to contain the liquid metal. The sonotrode was positioned at the top of the thin window of the quartz tube, and small pieces of Sn-30wt%Cu alloy were inserted inside the gap between the sonotrode and the quartz tube inner wall. The alloy was then melted in a specially designed furnace, with the temperature of the melt closely monitored by three K-type thermocouples placed at the top, middle and bottom of the thin window. A heat sink made of stainless steel rod was placed at the bottom of the quartz tube to create a thermal gradient. The details of the experiment are very similar to those described in [5, 6]. After reaching the target temperature (675 ºC in this case), a trigger unit was used to send a signal to the high speed X-ray imaging camera to start image acquisition and then, after 10 ms delay, to apply ultrasound to the melt. In this way, the whole process of ultrasound bubble nucleation, growth and propagation can be captured. The ultrasound was generated using an UP50H ultrasonic processor with a MS2 sonotrode (Hielscher ultrasound technology Ltd.). Ultrasound powers of 60 W and 100W were used in the experiment to create different bubble cloud with different characteristics.

2.2. High speed synchrotron X-ray imaging

The I12 Beamline has a wiggler source that provides an intense, high photon energy X-ray flux in the energy range 50-150 keV. Monochromatic and white beam modes are available. Filtered white beam was used to achieve high speed image acquisition up to 2000 frame per second (fps). (The intense X-ray beam was filtered with 4 mm of copper, to reduce heat load on the sample). The beamline's imaging system and Miro 310M high speed camera gave an image size of 800×1280 pixels with a spatial resolution of 4 μm × 4 μm per pixel. Due to the finite camera on-board memory, 4 s video was recorded in each acquisition. To correct for background noise and imperfections in the image path, flat field images (images acquired without the sample in the X-ray path), and background images (images acquired with the sample and sonotrode in the X-ray path but no ultrasound) were also obtained using the same sample setup, imaging frame rate and exposure time.

3. Results, analyses and discussion

3.1. Ultrasonic bubbles and bubble cloud

In total, 49 video sequences were acquired. Two typical video sequences were chosen to present here. Flat field correction, noise reduction and contrast/brightness adjustments for each video sequence were performed using the ImageJ software. Figure 1 shows three typical snapshots of the collective bubbles (bubble cloud) extracted from a video sequence captured using an ultrasonic power of 60 W. It can be seen that, in the area immediately below the sonotrode tip, there is a bright region which contains many interconnected bubbles. However below this region (1.5 – 3.2 mm below the sonotrode tip), there are many individual bubbles spread out in the view field.

Figure 2 shows a cloud of bubbles captured at 100 W ultrasound power. Individual bubbles cannot be clearly seen; instead, the bubbles seem to form a stream of interconnected bubble strings, indicating that, at 2000 fps, the individual bubbles moved too fast to be captured. However, at the location away

from the sonotrode such as the right bottom corner of Figure 2 (c) where the acoustic pressure is much lower than the area immediately blow the sonotrode tip, big, individual bubbles can still been seen.

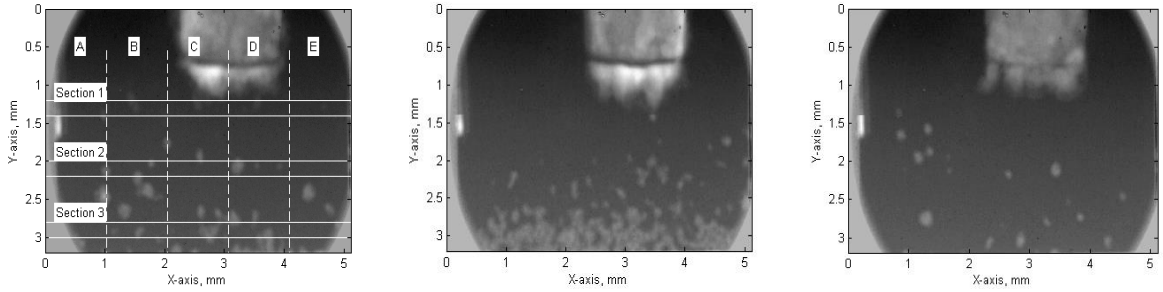

(a) (b) (c)

Figure 1 Images acquired from the liquid Sn-30%Cu alloy at 675 ˚C using an ultrasound power of 60 W, at (a) t0 = 5 ms (b) t1 = 25 ms (c) t2 = 45 ms, showing the ultrasonic bubble cloud immediately below the sonotrode tip and the individual bubbles at the location 1.5 – 3.2 mm below the sonotrode tip.

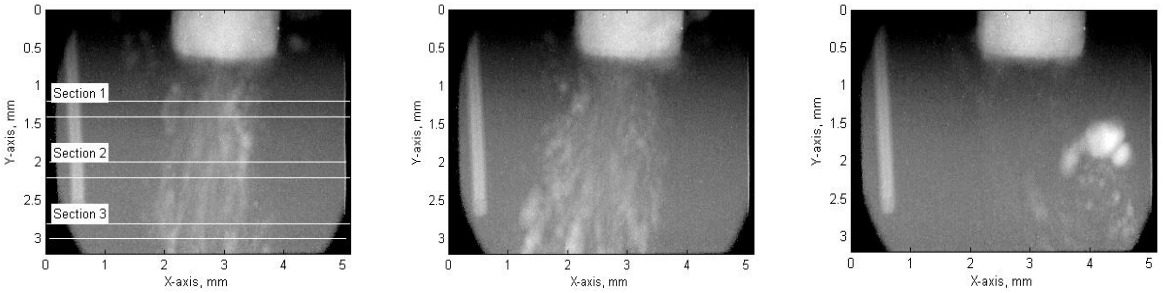

(a) (b) (c)

Figure 2 Images acquired from the liquid Sn-30%Cu alloy at 675 ˚C using an ultrasound power of 100 W, at (a) t0 = 25 ms (b) t1 = 35 ms (c) t2 = 45 ms, showing the ultrasonic bubble cloud.

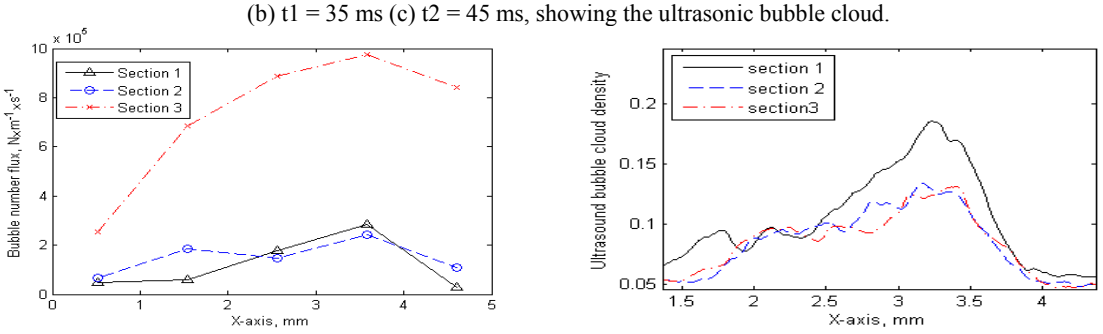

(a) (b)

Figure 3 (a) The bubble number density for the section 1, 2 and 3 showed Figure 1 (60 W), (b) the bubble cloud density for the section 1, 2 and 3 showed in Figure 2 (100 W).

3.2. The characteristics of the bubbles and bubble cloud

Comparing the images shown in Figure 1 and 2, it is seen that, at 60 W, especially in the region away from the sonotrode tip, the bubbles are clearly separated from each other, and have a near spherical morphology. Bubbles generated at 100 W were elongated and interconnected together to form a continuous bubble stream. To quantify the collective behaviour of the bubbles, i.e. the spatial distribution of the bubbles and bubble density, the numbers of bubbles passing though per unit length per unit time at a defined location were measured from each image in a sequence. Figure 1 (a) shows the chosen sections, labelled 1, 2 and 3, and each section was divided into 5 areas, marked A, B, C, D, and E, with each sectional width of 1.25 mm. A total of 100 images were measured in this way to obtain sufficient statistical data which is presented in Figure 3 (a). It clearly shows that there is a larger population of bubbles passing through Section 3. It also shows the maximum bubble flux occurred in the areas C and D in Figure 2 (a).

At 100 W, the interconnection of the bubbles makes it inaccurate to measure them individually. However, the interconnected bubbles formed a nearly continuous bubble cloud and the distribution of the bubble cloud (or more accurately the density of the bubbles) passing through a sectional length can be measured by the grey level along that section. Therefore, the bubble density along the same sections 1, 2 and 3 were calculated from 20 images for the 100 W case and presented in Figure 3(b).

Before the calculation of grey level, the noise and background of the raw images were already removed by subtracting the background image. Therefore, the remaining brightness was actually due to the ultrasound bubble cloud. By subtracting the background image (obtained from imaging the liquid metal only) from the flat field (without liquid metal), the difference in grey level was obtained and used as the baseline grey level. When bubble clouds were found in the sample, the grey level will be different to the grey level of the baseline. The ratio between the bubble cloud grey level and that of the baseline actually reflects the bubble density inside the sample. These ratios for the section 1, 2, and 3 for the case of 100 W were plotted in Figure 3 (b).

Although the data showed in Figure 3(a) is the bubble number density, while in Figure 3(b) they are the bubble densities, the trends are very similar, indicating that using the grey level to represent the bubble density can capture the essential characteristics of the bubble cloud distribution and flux behaviour.

3.3. Discussion

In most previous studies, the characteristics of ultrasonic bubbles and cavitation behaviours have been studied and analysed by methods such as high speed photography, foil testing, or acoustic emission spectrum measurement [8]. Those methods are generally not suitable for high temperature environments and opaque liquids. Some of them are invasive methods that may interrupt the ultrasound field, resulting in inaccurate measurement. In this paper, we demonstrated that by analysing the grey level of the captured images containing ultrasound bubbles or bubble clouds, the bubble cloud characteristics can be quantified.

4. Conclusion

In this paper, in-situ synchrotron X-ray imaging studies of ultrasound bubbles and bubble clouds in liquid Sn-30%Cu alloy were presented. By extracting statistical information from the acquired video sequences, the characteristics of ultrasonic bubbles and bubble cloud was quantified and discussed.

References

[1] Lauterborn W and Kurz T 2010 Physics of bubble oscillations *Reports on Progress in Physics* **73** 106501

[2] Zhang Y-n and Li S-c 2010 Direct numerical simulation of collective bubble behavior *Journal of Hydrodynamics, Ser. B* **22** 827-31

[3] Eskin G I 1997 Principles of ultrasonic treatment: Application for light alloys melts *Advanced Performance Materials* **4** 223-32

[4] Tan D, Lee T, Khong J, Connolley T, Fezzaa K and Mi J 2015 High-Speed Synchrotron X-ray Imaging Studies of the Ultrasound Shockwave and Enhanced Flow during Metal Solidification Processes *Metall and Mat Trans A* 1-11

[5] Lee T L, Khong J C, Fezzaa K and Mi J 2013 Ultrafast X-ray Imaging and Modelling of Ultrasonic Cavitations in Liquid Metal *Light Metals Technology 2013* **765** 190-4

[6] Mi J, Tan D and Lee T 2014 In Situ Synchrotron X-ray Study of Ultrasound Cavitation and Its Effect on Solidification Microstructures *Metall and Materi Trans B* 1-5

[7] Furtauer S, Li D, Cupid D and Flandorfer H 2013 The Cu-Sn phase diagram, Part I: New experimental results *Intermetallics* **34** 142-7

[8] Moholkar V S, Sable S P and Pandit A B 2000 Mapping the cavitation intensity in an ultrasonic bath using the acoustic emission *Aiche J.* **46** 684-94

Corrigendum: High speed synchrotron X-ray imaging of ultrasonic bubble cloud in liquid metal

C.Wang[1], D.Tang[1], W.Zhang[1], W. Du[1], T.Connolley[2], J. Mi[1]

[1]School of Engineering, University of Hull, Cottingham Road, Yorkshire, HU6 7RX, UK;
[2]Diamond Light Source, Didcot, Oxfordshire, OX11 0DE, UK

CORRIGENDUM TO: C.Wang et al 2015 J. Phys.: Conf. Ser. 656 012178

We would like to acknowledge the contribution of F. Wang, and D. Eskin to this work by adding their names as co-authors of the published article. The correct list of authors for the paper 'High speed synchrotron X-ray imaging of ultrasonic bubble cloud in liquid metal' is

C.Wang[1], D.Tang[1], W.Zhang[1], W. Du[1], T.Connolley[2], J. Mi[1], F. Wang[3], D. Eskin[3]

[1]School of Engineering, University of Hull, Cottingham Road, Yorkshire, HU6 7RX, UK;
[2]Diamond Light Source, Didcot, Oxfordshire, OX11 0DE, UK;
[3]Brunel Centre for Advanced Solidification Technology, Brunel University London, London, UB8 3PH, UK

We also would like to acknowledge the financial support from the EPSRC UltraCast project (Grant EP/L019884/1, EP/L019825/1, EP/L019965/1), and the award of the beamtime (experiment No. NT12131-1) by the UK Synchrotron X-ray facility, Diamond Light Source.